ARTICLE NO. 78-177R

Modeling of Momentum Transfer to a Surface by Laser-Supported Absorption Waves

J. P. Reilly,* A. Ballantyne,† and J. A. Woodroffe‡
Avco Everett Research Laboratory, Inc., Everett, Mass.

A simplified parametric model of the flowfield produced by impingement of a high-energy laser pulse onto a nonablative surface in a static environment is described. An attempt has been made to account for the two-dimensional effects arising out of the rarefaction structure within the laser-heated gases. An optimization model is developed to indicate the laser spot size, pulse width, and intensity dependencies of the efficiency of delivery of both impulse and mechanical energy to the target surface.

Nomenclature

A = area
C = sound speed
D = detonation velocity, defined in Eq. (5)
h = target thickness
I = impulse
K = nondimensional relaxation time ($=\tau_z/\tau_p$)
p = pressure
r = radial coordinate
R = blast wave radius
R_s = spot radius
t = time
u = radial velocity
$u(x)$ = axial velocity
v = velocity behind shock in LSC model
V_w = LSC wave speed
W = nondimensional particle velocity
x = axial coordinate
α = $(K\hat{\tau})$
γ = ratio of specific heats in plasma
γ_0 = ratio of specific heats in air
ρ = density
σ = target material density
τ_p = pulse length
τ_z = axial relaxation time
τ_{2D} = radial relaxation time
$\hat{\tau}$ = normalized pulse time ($=\tau_p/\tau_{2D}$)
τ_0 = pressure relaxation time
Φ_0 = incident laser flux intensity, W/cm^2

Subscripts

LSC = laser supported combustion condition
LSD = laser supported detonation condition
0 = ambient
r = condition behind rarefaction
s = surface, spot

Presented as Paper 78-177 at the AIAA 16th Aerospace Sciences Meeting, Huntsville, Ala., Jan. 16-18, 1978; submitted July 20, 1978; revision received April 2, 1979.

Index categories: Lasers; Nonsteady Aerodynamics; Shock Waves and Detonations.

*Vice President, Applied Technology Program; presently, Schafer Associates, Wakefield, Mass. Member AIAA.
†Senior Scientist. Member AIAA.
‡Principal Research Scientist. Member AIAA.

I. Introduction

THE dynamics of the plasma generated on a nonablative surface by a pulse of laser radiation is a function of incident flux level, ambient gas conditions above the surface, laser spot geometry, and pulse duration and shape. The objective of this paper is to describe a parametric model of the time history of the flowfield, and its consequent momentum transfer to the surface, induced by the laser flux. Although it uses approximate models of the gasdynamics, the model attempts to encompass the underlying physics of the processes involved.

The flowfield produced by the laser flux is generally divided into two regimes dependent upon flux intensity (Fig. 1). At flux levels slightly in excess of the plasma threshold, a subsonic laser supported combustion (LSC) wave will be generated.[1] This has been observed at flux levels in excess of 3×10^4 W/cm^2, for CO_2 lasers at 10.6 μm (Ref. 2). At substantially greater flux levels (greater than 10^7 W/cm^2), the short absorption length of the radiation allows a laser supported detonation (LSD) wave to form. At intermediate flux levels (10^6-10^7 W/cm^2), a transition occurs between these two states.

The strongly time-varying, three-dimensional nature of the flowfield makes it a particularly difficult problem to solve analytically. The cases described herein are limited, for the most part, to circular uniformly illuminated spots on the surface, with a simple step function flux history. The surface is assumed not to ablate to any significant degree; therefore, ablation thrust is not considered in the pressures exerted on the surface by the air plasma. The momentum transfer by pulsed lasers has been investigated by several authors. Pirri[4] developed a model for LSD waves using one-dimensional flow and blast wave scaling laws derived from similarity principles.[5] More recently, Holmes et al.[6] attempted to extend this to a quasi two-dimensional form, using a method of characteristics approach and blast decay laws. Ferriter et al.[7] have used both Pirri's one-dimensional approach and a computer simulation (LASNEX). The LSC structure has been less well described, as a result of its far greater mathematical complexity. Pirri et al.[8] and Boni et al.[9] have produced what is to date the most comprehensive descriptions of the one-dimensional flowfield.

II. Analytical Model of Surface Pressure Time History

Characteristic Time Scales and Initial Conditions

The surface pressure time histories for LSD waves have been described in terms of two characteristic time scales.[4,6] These are shown in the x-t diagrams of Fig. 2. The more important of these is the radial relaxation time, at which the leading edge of the radial rarefaction fan, produced by the

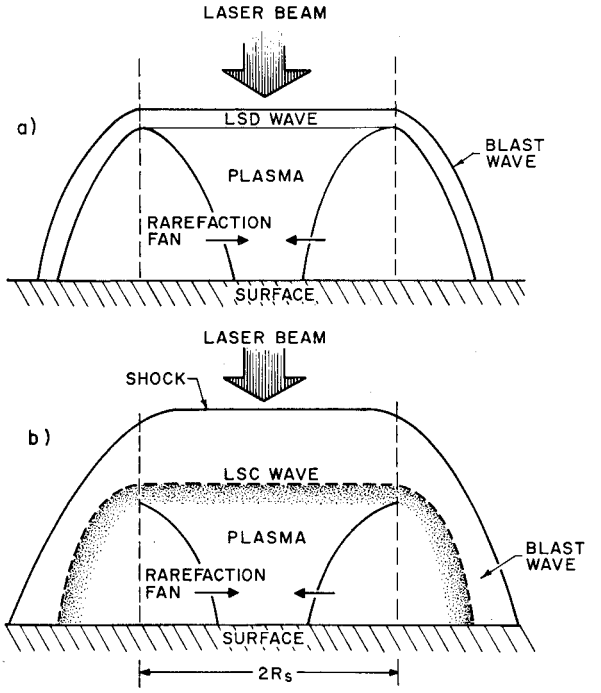

Fig. 1 Schematics of flow regimes: a) LSD wave; b) LSC wave.

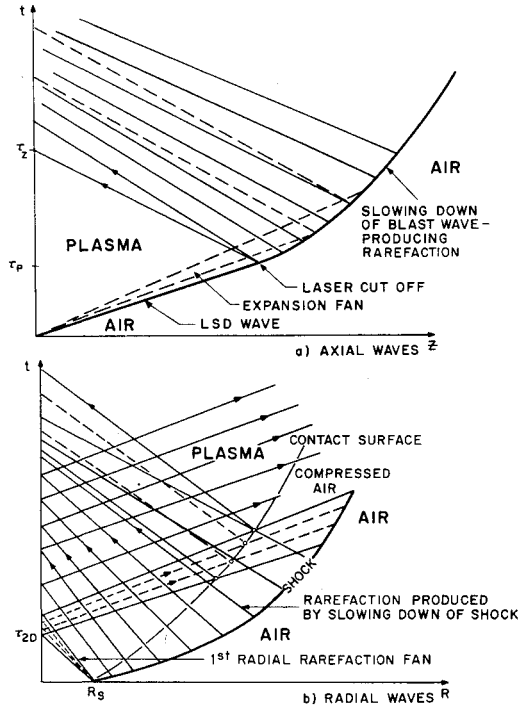

Fig. 2 *x-t* diagrams of constant flux LSD.

blast wave at the spot edge, reaches the spot center. This is given by

$$\tau_{2D} = R_s / C_s \tag{1}$$

where R_s is the laser spot radius and C_s is the sound speed in the hot plasma. On termination of the laser pulse at time τ_p, a rarefaction propagates backward from the detonation front, causing surface pressure relaxation subsequent to its arrival at time τ_z. The time history of the flowfield can thus be described in terms of the nondimensional times

$$\hat{\tau} = \tau_p / \tau_{2D} \tag{2}$$

$$K = \tau_z / \tau_p \tag{3}$$

Although not as well defined as for the LSD, similar time scales can be described for the LSC wave structure. The flowfield configurations for LSD or LSC waves are shown schematically in Fig. 1. The radial blast wave induces a radial rarefaction in the LSC, but its velocity toward the center is not as well characterized, as a result of the complex radial outflow pattern of the hot high-pressure plasma behind the wave. However, at the surface it would seem reasonable that boundary-layer effects produce a nearly stagnant zone across the spot. The radial relaxation time is thus assumed to have the same definition as for the LSD case [Eq. (1)].

The initial one-dimensional surface conditions ($t=0$) have been characterized by Raizer[3] for the LSD wave and by Boni et al.[9] for the LSC wave. Raizer's model assumes complete absorption of the laser flux in the detonation front, giving a surface pressure of

$$p_{s_{\mathrm{LSD}}} = \frac{[2(\gamma^2-1)]^{1/3}}{\gamma+1}\left[\frac{\gamma+1}{2\gamma}\right]^{2\gamma/\gamma-1} \rho_0^{1/3} \Phi_0^{2/3} \tag{4}$$

and a velocity of

$$D = [2(\gamma^2-1)\Phi_0/\rho_0]^{1/3} \tag{5}$$

where γ is the specific heat ratio of the gas ahead of the wave. An approximate solution has been obtained for the LSC wave[8] assuming uniform conditions behind the wave and between the percursor shock and the wave. The pressure and wave speeds are given in this case by

$$p_{s_{\mathrm{LSC}}} = \left[1-\frac{2W}{\gamma_0-1}\right]\left[\frac{\gamma_0+1}{2}\rho_0\right]^{1/3}\left[\frac{(\gamma-1)(\gamma+1)\Phi_p}{(\gamma+W)(\gamma_0-1-2W)}\right]^{1/3} \tag{6}$$

$$V_w = (W+1)\left[\frac{2(\gamma-1)(\gamma_0-1)}{(\gamma_0+1)(\gamma+W)(\gamma_0-1-2W)}\Phi_p/\rho_0\right]^{1/3} \tag{7}$$

where $\gamma_0 = 1.4$, $\gamma = 1.2$, and W is the nondimensionalized particle velocity through the wave given by

$$W = (V_w - v)/v \tag{8}$$

Φ_p is the absorbed laser flux which is, in general, less than Φ_0. Pirri et al.[8] gives the absorption to be between 80-90%.

The solution of the LSC conditions becomes a strong function of the absorption of the laser radiation by the plasma. For true LSC conditions $W \approx 0$. As the flux is increased to transition where the wave becomes sonic, it can be shown that the Chapman-Jouget condition (equivalent to a "weak" LSD wave structure) implies a value $W \approx 0.1$ (Ref. 8). The formation of a detonation-like structure at or near the transition flux intensities takes a finite time. This has been characterized by the time required for the initiating plasma to travel a distance equivalent to its absorption length. The predicted surface pressures for the LSC are roughly twice those of the LSD for a given flux intensity.

The surface sound speeds are given by:

$$C_{s_{\mathrm{LSD}}} = D/2 \tag{9}$$

$$C_{s_{\mathrm{LSC}}} = \left(\frac{\gamma p_{s_{\mathrm{LSC}}}}{\rho_0}\right)^{1/2}\left[\frac{W+1}{W}\frac{\gamma_0-1}{\gamma_0+1}\right]^{1/2} \tag{10}$$

$$\frac{C_{s_{\mathrm{LSC}}}}{C_{s_{\mathrm{LSD}}}} = \frac{\hat{\tau}_{\mathrm{LSC}}}{\hat{\tau}_{\mathrm{LSD}}} = \left[\frac{p_{s_{\mathrm{LSC}}}}{p_{s_{\mathrm{LSD}}}}\right]^{1/2}\left[\frac{\gamma_0-1}{\gamma_0+1}\frac{\gamma+1}{\gamma}\left(\frac{\gamma+1}{2\gamma}\right)^{2/\gamma-1}\frac{W+1}{W}\right]^{1/2} \tag{11}$$

Thus, for $W=0.04$, the ratio of sound speeds is approximately 2.4. The obvious problem with determination of LSC structure is the evaluation of W in terms of the radiation absorption. However, there is evidence to suggest that the pressure relaxation process occurs on a time scale commensurate with the sound speed being of approximately this value.[10]

The evaluation of τ_z for the LSD wave can be made in terms of the method of characteristics. The sound speed in the region behind the detonation wave has the form shown in Fig. 3. The resultant velocity of the rarefaction toward the surface subsequent to pulse termination is thus

$$\frac{dx}{dt}=c(x)-u(x)$$

where x is the distance of the leading rarefaction from the surface.

The characteristic for this rarefaction is:

$$\frac{2}{\gamma-1}c(x)-u(x)=\frac{D}{\gamma-1}.$$

Without detailing the algebra, the linear differential equation can be solved, giving

$$\tau_z=2\tau_p\left[\frac{2\gamma}{\gamma+1}\right]^{\frac{\gamma+1}{2(\gamma-1)}}$$

which gives a value of $K=3.2275$ for $\gamma=1.2$. This is longer than the approximate solution of $K=2.83$ obtained by Ferriter et al.,[7] as they considered the conditions behind the LSD wave to be uniformly $u(x)=0$ and $c(x)=\gamma D/(\gamma-1)$. The LSC wave, assuming uniform conditions behind the wave, gives an effective velocity of $C_{s_{LSC}}$. The distance that the wave has moved from the surface by pulse termination is $V_w\tau_p$. Thus,

$$\tau_z=\tau_p+V_w\tau_p/C_{s_{LSC}}$$

For $W=0.04$, this can be evaluated to be 1.47 τ_p, and for $W=0.1$ gives 1.96 τ_p.

Method of Characteristics Solution of Radial Rarefaction Fan

Holmes et al.[6] applied a method of characteristics approach to the solution of the pressure time history at various radial positions under the laser spot. They described the pressure decay in terms of a series of rarefactions bounding between centerline and contact surface causing a "staircase" decay. They ignored the effect of spherical or cylindrical expansion upon the blast wave, inducing a continuous motion of rarefactions toward the center, hence producing a continuous pressure decay. The present method then describes the pressure history in terms of the first radial rarefaction until time $t=\tau_{2D}$ and the subsequent decay in terms of blast decay scaling.

The continuity equation for cylindrical flow is given by:

$$\frac{\partial\rho}{\partial t}+u\frac{\partial\rho}{\partial r}+\rho\frac{\partial u}{\partial r}+\frac{\rho u}{r}=0 \qquad (12)$$

In order to solve this equation, the $\rho u/r$ term is neglected (i.e., quasi-one-dimensional). This would seem a reasonable approximation except at the spot center; hence, we expect inaccuracies in our analysis near the spot center. The characteristic solution is:

$$u\pm\frac{2}{\gamma-1}C=\text{constant}$$

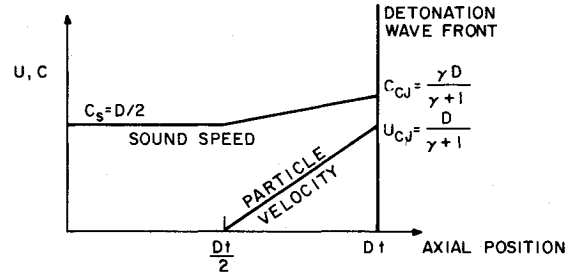

a) PARTICLE AND SOUND VELOCITY PROFILES BEHIND DETONATION WAVE (AT TIME t)

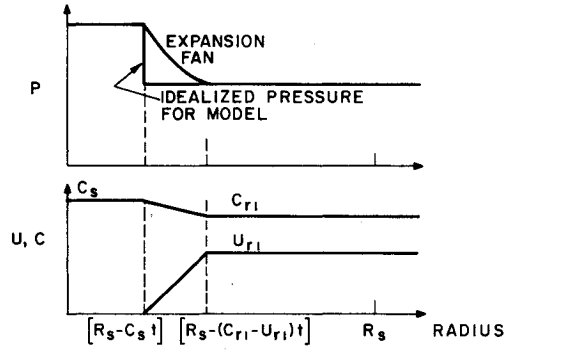

b) RADIAL PRESSURE AND VELOCITY PROFILES AT TIME t

Fig. 3 Axial and radial wave structures.

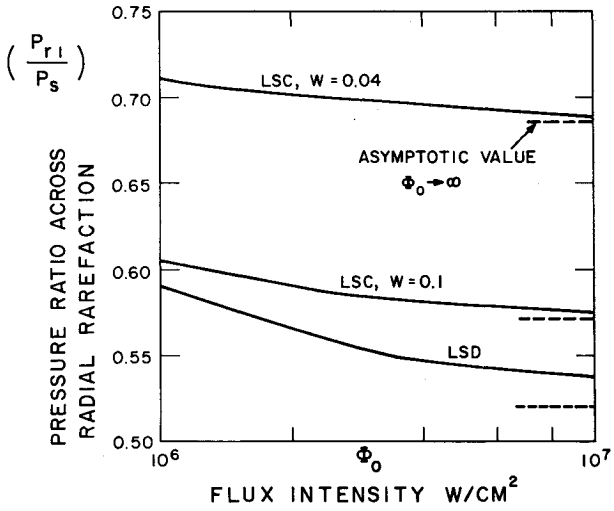

Fig. 4 Variation of radial fan pressure ratio with flux intensity and wave structure.

For the given rarefaction fan (see Fig. 3), the velocity behind the fan is given by:

$$u_r=\frac{2}{\gamma-1}C_s\left[1-\left(\frac{p_r}{p_s}\right)^{\frac{\gamma-1}{2\gamma}}\right] \qquad (13)$$

The shock tube equations give the velocity behind the fan as:

$$u_r=\left(\frac{\gamma_0 p_0}{\rho_0}\right)^{1/2}\left[\frac{p_r}{p_0}-1\right]\left[\frac{2/\gamma_0}{(\gamma_0+1)p_r/p_0+(\gamma_0-1)}\right]^{1/2} \qquad (14)$$

These two equations can be solved to give values of (p_r/p_s) as a function of p_s (and, consequently, Φ_p). The solution for the LSD in the flux intensity range 10^6-10^7 W/cm^2 is shown in Fig. 4. As can be seen, there is substantial variation in p_r/p_s within this flux range. The variation of (p_r/p_s) for the LSC

Table 1 Scaling laws (after Sedov[5])

	Pressure	Scale
Planar	$p=p_{ref}(t/\tau_{ref})^{-2/3}$	$X=X_{ref}(t/\tau_{ref})^{2/3}$
Cylindrical	$p=p_{ref}(t/\tau_{ref})^{-1}$	$R=R_{ref}(t/\tau_{ref})^{1/2}$
Powered cylindrical[a]	$p=p_{ref}(t/\tau_{ref})^{-1/2}$	$R=R_{ref}(t/\tau_{ref})^{3/4}$
Spherical	$p=p_{ref}(t/\tau_{ref})^{-6/5}$	$R=R_{ref}(t/\tau_{ref})^{2/5}$
Powered spherical[a]	$p=p_{ref}(t/\tau_{ref})^{-4/5}$	$R=R_{ref}(t/\tau_{ref})^{3/5}$

[a] Powered scaling laws refer to cases of linear energy deposition; i.e., constant flux Φ_0.

Table 2 Regimes of pressure decay scaling (circular spot)

I	
$\tau_p \le \tau_z \le \tau_{2D}$	Axial rarefaction arrives at surface before radial rarefaction reaches centerline
$0 \le \hat{\tau} \le K^{-1}$	Planar decay $\tau_z \le t \le \tau_{2D}$
	Spherical decay $\tau_{2D} \le t$
II	
$\tau_p \le \tau_{2D} \le \tau_z$	Radial rarefaction reaches centerline before axial rarefaction arrives at surface
$K^{-1} \le \hat{\tau} \le 1$	Spherical decay $\tau_{2D} \le t$
III	
$\tau_p \ge \tau_{2D}$	Radial rarefaction reaches centerline before axial rarefaction arrives at surface
$\hat{\tau} \ge 1$	Powered spherical decay $\tau_p \le t$

can be even more significant as a result of variation in W. As the exact variation in W is, in general, not known, it becomes difficult to model the LSC momentum transfer with any certainty. However, bounds can be placed in the values.

As W tends to zero, the analysis becomes physically unreasonable, with surface density tending to zero and sound speed to infinity. This is equivalent to no mass flow through the wave. The pressure ratio across the fan tends to unity and, as a result of the infinite sound speed, the impulse tends to zero.

Blast Decay Scaling Laws

The time history of the surface pressure is modeled in terms of self-similar scaling laws which provide a reasonably simple means of describing the pressure decay over the laser spot. The blast decay laws are taken to apply at times subsequent to the arrival of either the radial rarefaction at the center or the axial rarefaction at the surface. The geometry of the blast decay is dependent upon the relationship between τ_z and τ_{2D}. The pressure-time relationships for various geometries are given in Table 1.

The different regimes of pressure decay are characterized by the value of $\hat{\tau}$. There are essentially three ranges of $\hat{\tau}$; these are summarized in Table 2. The formulation of the momentum transfer is thus dependent upon the length of the pulse, relative to the two-dimensional relaxation time.

Model Formulation

The essence of the present formulation is that an attempt is made to include the effect of radial nonuniformity in the momentum transfer. The impulse delivered to the surface by a laser pulse is, by definition,

$$I=\int_0^{\tau_0}\int_A (p-p_0)\,dA\,dt \qquad (15)$$

where τ_0 is the time at which the surface pressure has relaxed to ambient conditions. It is to be noted that in the range of experimental conditions for flux intensities of the order of 10^6-10^7 W/cm s, the effect of ignoring the term $-p_0\tau_0 A$ can be significant. Several authors have evaluated impulse as

$$I=\int_0^{\tau_0}\int_A p\,dA\,dt$$

For extremely high ratios p_s/p_0 this is correct, but the contribution to the effective impulse by $(-p_0\tau_0 A)$ can be of order 20-40% for flux intensities corresponding to surface pressure ratios (p_s/p_0) of up to 60.

The model described here specifically relates to the momentum transferred to the laser-illuminated region of surface (A_s). This is not the total impulse delivered to the surface. The radial spread of the blast wave results in an increased area for impulse pressure to act upon. However, no attempt has been made in this paper to consider this contribution to total impulse delivery.

The model described here, for calculation purposes, treats the radial rarefaction fan as being infinitesimally thin. In terms of contribution to the total impulse, the effect of ignoring the additional impulse, in terms of the assumed self-similar decay subsequent to fan arrival at the centerline, accounts for only 1% at most. Within the limits of overall accuracy allowable by the conceptual approach of the model, this is insignificant, and for simplicity, ignorable. The radial flow model thus takes the form illustrated in Fig. 3.

Regimes II and III are somewhat simply described. The impulsive contribution up to $t=\tau_{2D}$ is given by:

$$I_1=\pi R_s^2\int_0^{\tau_{2D}} p_s(1-t/\tau_{2D})^2\,dt$$

$$+\pi R_s^2\int_0^{\tau_{2D}} p_r[1-(1-t/\tau_{2D})]^2\,dt$$

where the first term corresponds to the region in front of the rarefaction, and the second to the region behind it. On integration, this gives

$$I_1=\tfrac{1}{3}\pi R_s^2\tau_{2D}p_s[1+2(p_r/p_s)] \qquad (16)$$

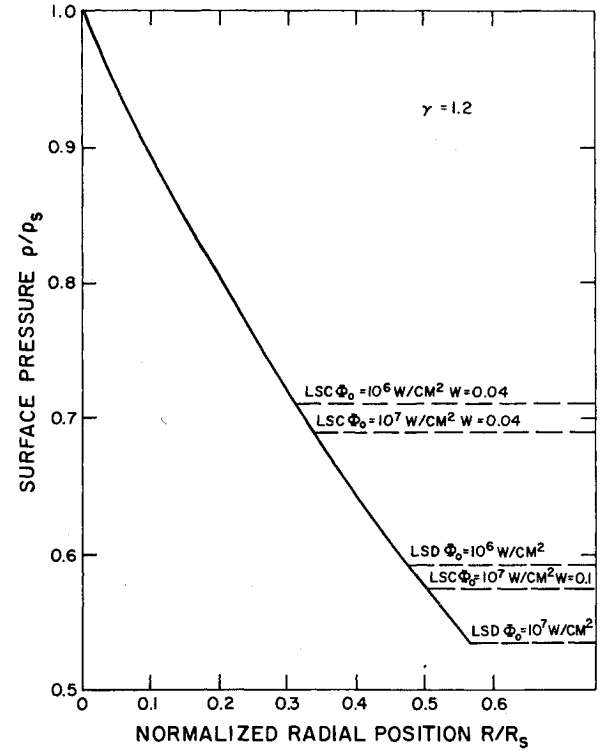

Fig. 5 Pressure profile across rarefaction wave at $t=\tau_{2D}$.

The subsequent time history is then given by a blast wave decay. At this point, the question arises as to the initial pressure for the decay process. Obviously, as far as the finite width rarefaction fan is concerned, the centerline pressure remains p_s at $t=\tau_{2D}$. However, considering the entire laser-illuminated spot, the majority of the area is at a pressure p_r. Examination of the fan structure (Fig. 5) shows that greater than 70% of the area is at pressure p_r. This is, of course, neglecting the additional rarefaction effects produced by the expansion of the radial blast wave, which is a consequence of the simplified quasi-one-dimensional characteristics solution. An interesting comparison is that of the computer simulation of Ferriter et al.[7] (Fig. 6). The pressure decay predicted by their results would appear more in keeping with the postrarefaction pressure p_r. On this basis, the subsequent momentum transfer is given by:

$$I_2/A_s=\int_{\tau_{2D}}^{\tau_0} p_r\left(\frac{t}{\tau_{2D}}\right)^{-6/5}\mathrm{d}t \quad (K^{-1}\le\hat{\tau}\le 1) \tag{17a}$$

and

$$I_2/A_s=\int_{\tau_{2D}}^{\tau_p} p_r\left(\frac{t}{\tau_{2D}}\right)^{-4/5}\mathrm{d}t + \int_{\tau_p}^{\tau_0} p_r\hat{\tau}^{-4/5}\left(\frac{t}{\tau_p}\right)^{-6/5}\mathrm{d}t \quad (1\le\hat{\tau}\le\hat{\tau}_{\max}) \tag{17b}$$

where the decay time, τ_0, is given by

$$\tau_0=(p_r/p_0)^{5/6}\tau_{2D} \qquad (K^{-1}\le\tau\le 1)$$

$$\tau_0=(p_r/p_0)^{5/6}\tau_p\hat{\tau}^{-2/3} \qquad (1\le\hat{\tau})$$

The maximum pulse length, $\tau_{\max}$, is such that the powered spherical blast decays to ambient conditions at the point of pulse termination. Any subsequent power addition is wasted. Thus,

$$\hat{\tau}_{\max}=(p_r/p_0)^{5/4}$$

Without detailing the algebra, the total (area-integrated) impulses, given by

$$I=(I_1+I_2-p_0\tau_0A_s)$$

become, in normalized form,

$$\frac{I}{[A_sp_s\tau_p]}=\frac{1}{\hat{\tau}}\left[\frac{1}{3}\left(1+2\left(\frac{p_r}{p_s}\right)\right)+5\left(\frac{p_r}{p_s}\right)\left[1-\left(\frac{p_s}{p_0}\right)^{-1/6}\right]\right] - \frac{1}{\hat{\tau}}\left(\frac{p_r}{p_s}\right)^{5/6}\left(\frac{p_s}{p_0}\right)^{-1/6} \qquad (K^{-1}\le\hat{\tau}\le 1) \tag{18a}$$

and

$$\frac{I}{[A_sp_s\tau_p]}=\frac{1}{\hat{\tau}}\left[\frac{1}{3}\left(1+2\left(\frac{p_r}{p_s}\right)\right)+5\left(\frac{p_r}{p_s}\right)(\hat{\tau}^{1/5}-1)\right] +5\left(\frac{p_r}{p_s}\right)\hat{\tau}^{-4/5}\left[1-\hat{\tau}^{2/15}\left(\frac{p_r}{p_0}\right)^{-1/6}\right] -\hat{\tau}^{-2/3}\left(\frac{p_r}{p_s}\right)^{5/6}\left(\frac{p_s}{p_0}\right)^{-1/6} \qquad (1\le\hat{\tau}\le\hat{\tau}_{\max}) \tag{18b}$$

It has been suggested that cylindrical blast model is applicable for $\tau\ge\tau_{2D}$.[4] For completeness, in the absence of any precise evidence to the nature of the decay process, the cylindrical

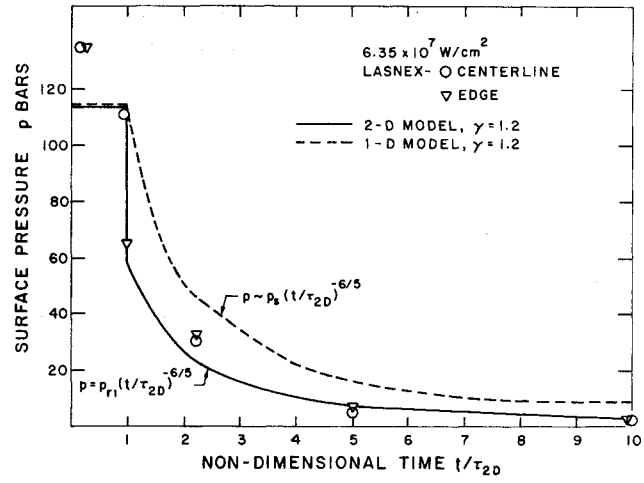

Fig. 6 Comparison of two-dimensional model with LASNEX[7]—pressure decay.

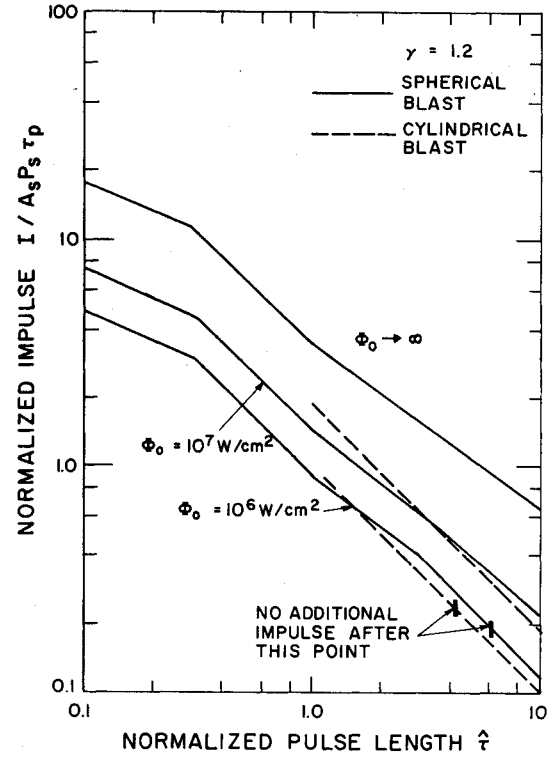

Fig. 7 Normalized impulse over spot for two-dimensional model of LSD.

solution of the preceding formulation is given. Thus,

$$\frac{I}{[A_sp_s\tau_p]}=\frac{1}{\hat{\tau}}\left[\frac{1}{3}\left(1+2\left(\frac{p_r}{p_s}\right)\right)\right] +\frac{1}{\hat{\tau}}\left[\left(\frac{p_r}{p_s}\right)\ln\left(\frac{p_r}{p_0}\right)-\left(\frac{p_r}{p_s}\right)\right] \qquad (1\le\hat{\tau}) \tag{19}$$

The short pulse regime produces a planar decay in the region inside the rarefaction fan. The interaction of the two rarefactions is not clearly defined. However, it can be shown that the sound speed behind the fan is given by:

$$C_s(p_r/p_s)^{\gamma-1/2\gamma}$$

which, for the pressure ratios of interest, is only slightly less than C_s. The assumption for this part of the model is that the

planar decay takes place over the entire laser spot, while the rarefaction continues inward at an unchanged velocity, with no change in pressure ratio across the fan. The pressure integral thus becomes, in a manner similar to Eq. (4),

$$I_I/A_S = \int_0^{\tau_z} \left\{p_S(1-t/\tau_{2D})^2 + p_r[1-(1-t/\tau_{2D})^2]\right\}dt$$

$$+ \int_{\tau_z}^{\tau_{2D}} \left\{p_s\left(\frac{t}{\tau_z}\right)^{-2/3}(1-t/\tau_{2D})^2\right.$$

$$\left. + p_r(t/\tau_z)^{-2/3}[1-(1-t/\tau_{2D})^2]\right\}dt$$

This is followed by a spherical decay at initial pressure $p_r(K\hat{\tau})^{2/3}$. Thus,

$$\frac{I}{[A_s p_s \tau_p]} = K\left[1-\left(1-\frac{p_r}{p_s}\right)\left(\alpha-\frac{1}{3}\alpha^2\right)+3\left(\frac{p_r}{p_s}\right)\left(\alpha^{-1/3}-1\right)\right]$$

$$+3K\left(1-\frac{p_r}{p_s}\right)\left[\alpha^{-1/3}-1-\frac{\alpha}{2}\left(\alpha^{-4/3}-1\right)+\frac{\alpha^2}{7}\left(\alpha^{-7/3}-1\right)\right]$$

$$+5K\left(\frac{p_r}{p_s}\right)\alpha^{-1/3}\left[1-\alpha^{-1/9}\left(\frac{p_r}{p_0}\right)^{-1/6}\right]$$

$$-K\left(\frac{p_r}{p_s}\right)^{5/6}\left(\frac{p_s}{p_0}\right)^{-1/6}\alpha^{-4/9} \qquad (20)$$

where $\alpha = (K\hat{\tau})$.

This expression is valid until $\hat{\tau}$ becomes sufficiently small, that ambient pressure is reached during the planar decay period. The bounding value of $\hat{\tau}$ is, therefore,

$$\hat{\tau} \geq K^{-1}(p_r/p_0)^{-3/2}$$

For $\Phi_0 = 10^6$ W/cm^2 and LSD conditions, this gives a lower bound of 0.035. The impulsive coupling to the surface is illustrated in Fig. 7 for an LSD wave. As the divisor of the normalized impulse is a measure of the delivered laser energy, the ordinate becomes a measure of efficiency of impulsive delivery to a surface. Thus, it is clear that short pulse lengths and high flux levels produce more efficient impulsive loading. The cylindrical and spherical models can be seen to differ up to 25% in the range of $\hat{\tau}$ illustrated. The cutoff points on the $\Phi_0 = 10^6$ W^2/cm^2 curves correspond to the pressure decaying to ambient conditions at the same time as the laser pulse terminates. Any laser energy deposited after this time is wasted, as it does not contribute to impulse. The comparison of LSD and LSC behavior in the transition region of flux intensities between 10^6-10^7 W/cm^2 is made difficult by the lack of precise information concerning wave structure. However, it is useful to consider the two limits of the LSC model behavior. From Pirri et al.,[8] the predicted surface pressure corresponds roughly to $W \simeq 0.04$. At transition, the effectively overdriven detonation wave gives $W \simeq 0.104$. The use of the nondimensional impulse is not possible here, as the surface pressures are different. The comparison is thus in terms of an effective impluse pressure $I/A_s\tau_p$. The two models are compared in Fig. 8. At a flux of 10^6 W/cm^2, the LSC indicates a higher impulse than the LSD over the entire range of $\hat{\tau}$, ranging from 10-45%. At 10^7 W/cm^2, the two values of W indicate substantial differences for the LSC, being especially noticeable at short pulse times. Again, the LSD gives a smaller value of impulse.

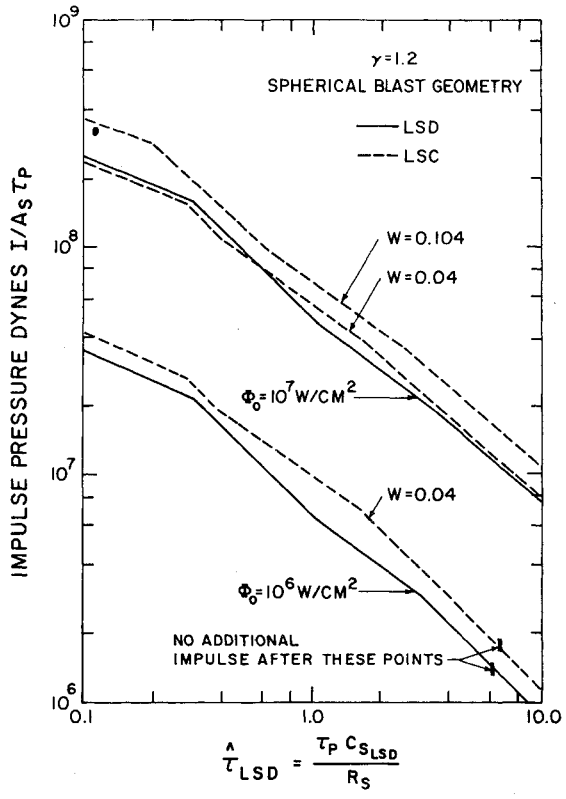

Fig. 8 Comparison of LSC and LSD two-dimensional models in the transition range of flux intensities: spot averaged impulse.

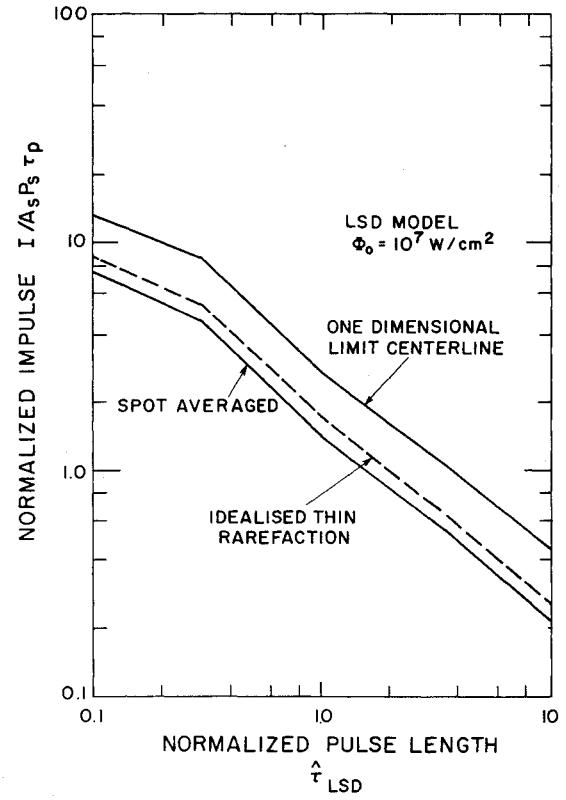

Fig. 9 Comparison of centerline impulses for LSD.

The Centerline Impulse

The preceding formulation is constructed in terms of the pressure behind the radial rarefaction fan and the assumption of infinitesimal fan thickness. Obviously, this is not so. As illustrated in Fig. 5, the rarefraction varies between 0.3 and 0.55 of the spot radius in width at the $t = \tau_{2D}$. The decay of pressure on the centerline must, therefore, be from an initial pressure of p_s not p_r. In applying a self-similar blast decay

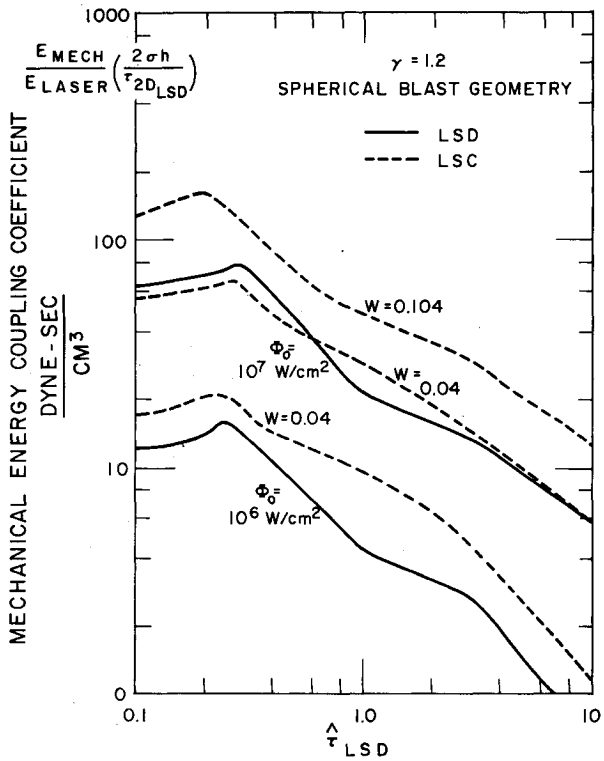

Fig. 10 Mechanical energy coupling efficiency for LSC and LSD two-dimensional models.

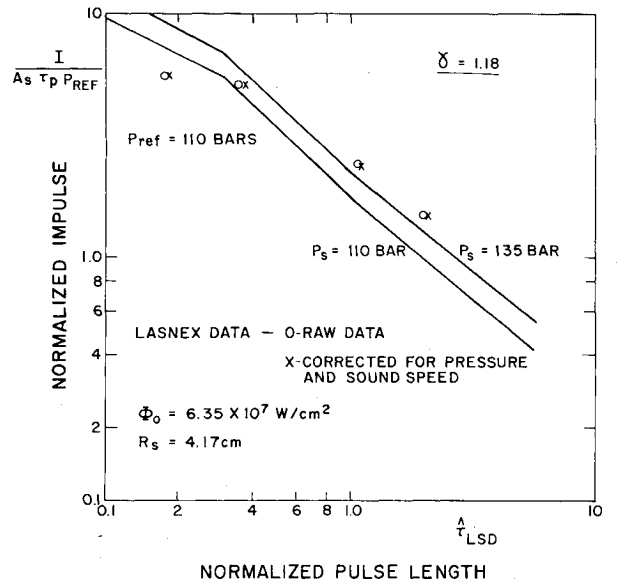

Fig. 11 Comparison of impulse predictions of LSD two-dimensional model with LASNEX.[7]

uniformly over the spot, we are violating this initial condition. There appears to be no easy answer to this problem, but as an upper bound, the one-dimensional limit appears to give an estimate of centerline impulsive intensity. Thus, for example, the one-dimensional equivalent to Eq. (18a) gives

$$\frac{(I/A)}{p_s\tau_p} = \frac{1}{\hat{\tau}}\left[1+5\left[1-\left(\frac{p_s}{p_0}\right)^{-1/6}\right]-\left(\frac{p_s}{p_0}\right)^{-1/6}\right]$$

The difference between the spot-averaged and centerline limits can be seen, in Fig. 9, for an LSD structure at 10^7 W/cm^2. The ratio of impulses in these two models approximately corresponds to the pressure ratio (p_s/p_r).

The centerline impulse may possibly be represented by an infinitesimally thin fan and decay starting from the rarefaction pressure p_r. This gives an impulse, which lies between the spot-averaged and one-dimensional values. The algorithms for this are, thus, similar to Eqs. (18-20), with the first term replaced by unity. Thus, for example, Eq. (18a) gives

$$\frac{(I/A)_{\text{center}}}{A_s\tau_p} = \hat{\tau}^{-1}\left[1+5\left(\frac{p_r}{p_s}\right)\left[1-\left(\frac{p_r}{p_0}\right)^{-1/6}\right]\right.$$
$$\left.-\left(\frac{p_r}{p_s}\right)^{5/6}\left(\frac{p_s}{p_0}\right)^{-1/6}\right]$$

Efficiency of Impulse Delivery

The crudest measure of the efficiency of impulse delivery is the coupling coefficient defined by:

$$\frac{I_s}{E_{\text{laser}}} = \left[\frac{I_s}{A_s p_s \tau_p}\frac{p_s}{\Phi_0}\right]$$

As p_s is proportional to $\Phi_0^{2/3}$ for both LSD and LSC waves, the coupling coefficient is such that

$$\frac{I_s}{E_{\text{laser}}} = \text{const.}\left[\frac{I_s}{A_s p_s \tau_p}\right]\Phi_0^{-1/3}$$

From this, it would appear that there is no obvious optimum pulse length, $\hat{\tau}$, for efficient delivery. However, we require an optimum mechanical energy delivery to the surface. We can define the mechanical energy by:

$$E_{\text{mech}} = 1/2\sigma h A\left[\frac{I_s}{A\sigma h}\right]^2$$

where $I_s/A\sigma h$ is the effective velocity imparted to the surface beneath the spot. Thus, we have a coupling coefficient

$$\frac{E_{\text{mech}}}{E_{\text{laser}}} = 1/2(\sigma h)^{-1}\left[\frac{I_s}{A_s p_s \tau_p}\right]^2\frac{\tau_p p_s^2}{\Phi_0}$$

Therefore, we can write

$$\frac{E_{\text{mech}}}{E_{\text{laser}}}\left(\frac{2\sigma h}{\tau_{2D_{\text{LSD}}}}\right) = \left[\frac{I_s}{A_s\tau_p}\right]^2\frac{\hat{\tau}_{\text{LSD}}}{\Phi_0} \tag{21}$$

This relationship is plotted for the same condition as given in Fig. 10. As can be seen, an optimum pulse length does exist. Although there is some slight variation with flux and LSC particle velocity, the optimum pulse length lies below $\hat{\tau} \approx 0.5$. It should be noted that the LSC structure, in general, provides a higher mechanical coupling than the LSD.

III. Comparison of LSD Calculations with LASNEX Code

Ferriter et al.[7] utilized the LASNEX code to provide calculation of spot impulse at a flux intensity of 6.35×10^7 W/cm^2. Their results are shown in Fig. 11. The data correspond to a calculated surface pressure of 110 bars. As can be seen, there is a significant difference between the prediction of the present model and these of LASNEX. However, this is due in part to discrepancies in the calculated surface pressure and the value indicated by LASNEX; 135 bars as opposed to 110 bars, as given by Eq. (5). Ferriter et al. explain this discrepancy in terms of their initial conditions for the computation. They assumed a 0.1-cm-thick zone of hot air above the surface at 1.5 eV as starting conditions. Re-evaluating the present model in terms of a 135-bar initial pressure and a higher sound speed gives much better agreement. At long pulse times, the LASNEX predictions are approximately 15% higher than the two-dimensional model, whereas at short pulse lengths, they are low by about 35%.

This latter result would again appear to relate to their initial conditions, as the axial relaxation time is only 70% of its predicted value, producing a more rapid pressure decay.

On the whole, it would appear that satisfactory agreement has been obtained between the LASNEX computer code and the present algorithmic two-dimensional model.

IV. Conclusions

A simplified, algorithmic model of momentum transfer to a plane nonablating surface has been developed. It can be used to describe both LSD and LSC wave structures in terms of nondimensional pulse lengths and relaxation times. The LSD compares well with computer predictions at high flux levels (in excess of 10^7 W/cm^2). Although lacking precise definition at the present time, the LSC structure can be described in a similar manner to the LSD, given knowledge of its radiative properties (which imply a value of W). In general, the LSC structure produces a higher impulsive coupling than the LSD for a given flux intensity.

The optimum mechanical energy coupling, provided by the laser pulse, has been calculated to be in the range $0.2 \leq \hat{\tau}_{LSD} \leq 0.3$ for a flux intensity between 10^6-10^7 W/cm^2. For maximum energy transfer to the target, the pulse length may be tailored with beam diameter and flux intensity to be in this range.

It has been found that the model described here has reasonable agreement with the observed impulse data published in Ref. 10, and the reader is referred to that paper for further information.

Acknowledgments

This work was supported by the Avco Independent Research and Development Program. The authors would like to thank A. N. Pirri, D. A. Reilly, G. W. Sutton, and T. Tucker for their useful discussions during the course of this work.

References

[1] Raizer, Yu P., "Heating of a Gas by a Powerful Light Pulse," *Soviet Physics JETP*, Vol. 21, Nov. 1965, pp. 1009-1017.

[2] Klosterman, E. L. and Byron, S. R., "Measurement of Subsonic Laser Absorption Wave Propagation at 10.6μm," *Journal of Applied Physics*, Vol. 45, Nov. 1974, pp. 4751-4759.

[3] Raizer, Yu P., "Subsonic Propagation of a Light Spark and Threshold Conditions for the Maintenance of Plasma by Radiation," *Soviet Physics JETP*, Vol. 31, Dec. 1970, pp. 1148-1154.

[4] Pirri, A. N., "Theory of Momentum Transfer to a Surface with a High Power Laser," *The Physics of Fluids*, Vol. 16, Sept. 1973, pp. 1435-1440.

[5] Sedov, L. I., *Similarity and Dimensional Methods in Mechanics*, Academic Press, New York, 1959.

[6] Holmes, B. S., Tarver, C., Erlich, D. C., Lindberg, H. E., "The Mechanical Loads from LSD Waves and their Simulation," Stanford Research Institute, Final Report Under Contract F29601-74-C-0051, March 1976.

[7] Ferriter, N., Maiden, D. E., Winslow, A. M., and Fleck, J. A., "Laser Beam Optimization for Momentum Transfer by Laser Supported Detonation Waves," *AIAA Journal*, Vol. 5, Nov. 1977, pp. 1597-1603.

[8] Pirri, A. N., Root, R. C., and Wu, P.K.S., "Plasma Energy Transfer to Metal Surfaces Irradiated by Pulsed Lasers," *AIAA Journal*, Vol. 16, Dec. 1978, p. 1296.

[9] Boni, A. A., Su, F. Y., Thomas, P. D., and Musal, H. M., "Theoretical Study of Laser-Target Interactions," Final Tech. Rept., SAI 77-77-567-LJ, Science Application Inc., LaJolla, Calif., May 1977.

[10] Woodroffe, J. A., Stankevics, J.O.A., Ballantyne, A., and Reilly, J. P., "Laser Generated Impulse on a Surface in Supersonic Flow." *AIAA Journal*, to be published.